

Augmented Multi-Subarray Dilated Nested Array with Enhanced Degrees of Freedom and Reduced Mutual Coupling

Hua Chen, *Senior Member, IEEE*, Hongguang Lin, Wei Liu, *Senior Member, IEEE*, Qing Wang, *Member, IEEE*, Qing Shen, *Senior Member, IEEE* and Gang Wang, *Senior Member, IEEE*

Abstract—Sparse linear arrays (SLAs) can be designed in a systematic way, with the ability for underdetermined DOA estimation where a greater number of sources can be detected than that of sensors. In this paper, as the first stage, a new systematic design named multi-subarray dilated nested array (MDNA), whose difference co-array (DCA) can be proved to be hole-free, is firstly proposed by introducing a sparse ULA and multiple identical dense ULAs with appropriate sub-ULA spacings. The MDNA will degenerate into the nested array under specific conditions, and the uniform degrees of freedom (uDOFs) of MDNA is larger than that of its parent nested array. On the basis of MDNA, to reduce the mutual coupling effect, an augmented multi-subarray dilated nested array (AMDNA) is constructed by migrating some elements of the dense segments of MDNA, without reducing the number of uDOFs. Several theoretical properties of the proposed array structures are proved, and simulation results are provided to demonstrate the effectiveness and superiority of the proposed AMDNA over some existing sparse arrays.

Index Terms—Sparse array, DOA estimation, nested array, multi-subarray dilated nested array, augmented multi-subarray dilated nested array.

I. INTRODUCTION

Uniform linear arrays (ULAs) are widely used in array processing applications [1], which with N equidistant physical sensors can detect $N-1$ sources using either subspace-based methods [2] or sparsity-based methods [3]. Meanwhile, the spacing between adjacent sensors in ULAs is usually

This work was supported by the Zhejiang Provincial Natural Science Foundation of China under Grants LY23F010003 and LR20F010001, by the National Natural Science Foundation of China under Grants 62001256, 62271052, U20A20162 and 62222109, and the UK Engineering and Physical Sciences Research Council (EPSRC) under Grants EP/V009419/1 and EP/V009419/2, and the Key Research and Development Program of Tibet Autonomous Region, and the Science and Technology Major Project of Tibetan Autonomous Region of China under Grant XZ202201ZD0006G03. For the purpose of open access, the author(s) has applied a Creative Commons Attribution (CC BY) license to any Accepted Manuscript version arising. (*Corresponding author: Hua Chen*)

Hua Chen, Hongguang Lin and Gang Wang are Faculty of Electrical Engineering and Computer Science, Ningbo University, China. (e-mail: dkchenhua0714@hotmail.com; wanggang@nbu.edu.cn)

Hua Chen is also with the Zhejiang Key Laboratory of Mobile Network Application Technology, Ningbo 315211, P. R. China.

Wei Liu is with the School of Electronic Engineering and Computer Science, Queen Mary University of London, London E1 4NS, UK. (e-mail: wliu.eee@gmail.com)

Qing Wang is with the School of Electronic Informatin Engineering, Tianjin University, Tianjin 300072, China. (e-mail:wqelaine@tju.edu.cn)

Qing Shen is with School of Information and Electronics, Beijing Institute of Technology, China. (e-mail:qing-shen@outlook.com)

confined within $\lambda/2$ to circumvent spatial aliasing, where λ denotes the operating wavelength. This rather limited inter-element spacing inevitably results in strong mutual coupling (MC) effects, which has a negative impact on direction of arrival (DOA) estimation performance if not dealt with properly.

As compared to ULAs, sparse linear arrays (SLAs) have attracted strong interest over the past decade [4]–[16]. By vectorizing the covariance matrix of the observed array data, an increased number of degrees of freedom (DOFs) is achieved based on the idea of difference co-array (DCA), which makes it possible for underdetermined DOA estimation [17], where a greater number of sources can be detected than that of physical sensors. Early representative configurations of sparse arrays are the minimum redundancy array (MRA) [8] and minimum hole array (MHA) [9]. Although MRA and MHA are effective in increasing the number of achievable DOFs, they don't have closed-form expressions for sensor locations as well as the number of DOFs. Therefore, it is challenging to design MRAs and MHAs for a large number of sensors, which limits their applications in practice.

On the other hand, nested arrays (NAs) [10]–[12] and coprime arrays (CPAs) [13]–[16], [18] can be systematically designed with closed-form expressions for the number of achievable DOFs, as compared to the shortcomings of MRA and MHA. By increasing the spacing of elements, nested arrays obtained by combining two or more ULAs can provide $O(N^2)$ DOFs with N physical sensors. Especially by interleaving two ULAs in different ways, a two-level nested array (NA) can achieve a hole-free virtual DCA.

However, the NAs are less resistant to MC due to the dense ULA employed in the physical array, while the CPAs can reduce MC between elements. Following the ideas of CPAs and NAs, a variety of new sparse arrays including evolutionary NAs [19]–[23] and CPAs [24]–[28] have been developed. For nested-type evolutionary arrays, the proposed one-side extended nested array (OS-ENA) and two-side extended nested array (TS-ENA) are proposed in [19], which only focus on large DOFs, ignoring the strong MC of the extended NAs. To alleviate the MC effect while retaining advantages of the parent NA, a (second-order) super nested array (2-SNA) is designed to reduce the number of sensor pairs with small inter-sensor spacings [20], whose key design idea is to rearrange the dense ULA portion of the parent NA. Then, an extension of 2-SNA, named as high-order SNA is proposed in [21], which can maintain the positive properties of 2-SNA while further

reducing the MC effect. In addition, by dividing the dense sub-ULA of the parent NA into two or four parts, augmented nested arrays (ANAs) [22] are configured with four different structural designs, namely ANAI-1, ANAI-2, ANAI-1 and ANAI-2, where the MC of the first two arrays is not significantly reduced, while the latter two need complex conditions to meet the requirements of the hole-free virtual DCA. In [23], composed of three sub-ULAs, the dilated nested array (DNA), is developed, and further evolves into the super DNA (SDNA) with effective highest-order extension procedures that alleviate the first three critical weight functions.

For coprime-type evolutionary arrays, two generalized CPAs named as the coprime array with compressed inter-element spacing (CACIS) and coprime array with displaced subarrays (CADiS) have been suggested in [24], where the former employing the compressed inter-sensor spacing has stronger MC effects than parent CPA, while the latter is unable to produce the consecutive lags connected the negative and positive co-arrays. Then, aiming to further increase the uDOFs of CPA and at the same time reduce the MC effects, a series of improved CPAs, such as thinned coprime array (TCA) [25], relocating ECA (RECA) [26], extended padded coprime array (ePCA) [27] and enhanced and generalized coprime array (EGCA) [28] have been designed by dealing with the redundant sensors in the parent CPA or filling the holes in the corresponding DCA.

In general, the above-mentioned coprime-type evolutionary arrays can increase the uDOFs of the CPA, but still cannot catch with that of the nested-type evolutionary arrays, despite reduced MC. Besides, in [29], the minimum inter-sensor spacing constraint (MISC) array is introduced by constructing three sparse ULAs and two separate sensors with appropriate inter-element spacing, with the array configured in terms of the inter-element spacing set. With an arbitrary number of sub-ULAs, a new design principle called ULA fitting is proposed [30] for SLAs, whose design requirements (like large uDOFs and low MC) are transferred into pseudo-polynomial equation, which has found its application in MIMO radar [31].

In this paper, a new array scheme called multi-subarray dilated nested array (MDNA) is first introduced, which maintains all beneficial properties of the parent NA. By introducing a sparse ULA and multiple identical dense ULAs with appropriate sub-ULA spacings, the DOFs of the MDNA with hole-free DCA is enhanced compared to that of the parent NA. By systematically redistributing the elements of the multiple identical dense ULAs of the MDNA, we finally propose a new array configuration called augmented MDNA (AMDNA). Compared with the MDNA, the AMDNA greatly reduces the MC effects without decreasing the uDOFs. The contributions of this paper are summarized as below:

1) A novel structure with hole-free DCA, referred to as MDNA, is proposed with NA being one of its special case. After investigating the performance limit of the MDNA by optimizing its design settings, increased number of uDOFs can be achieved compared with existing structures.

2) Considering the MC effect, a displaced arrangement to the dense elements of MDNA is introduced to obtain the configuration of AMDNA, and it is proved that AMDNA has almost the same number of uDOFs but less MC compared

with the MDNA.

The rest of this paper is organized as follows. Sparse array processing with DCA generation and MC models are briefly reviewed in Section II. The proposed MDNA and AMDNA are presented respectively in Sections III and IV. In Section V, performance of the proposed MDNA and AMDNA is demonstrated through computer simulations, and conclusions are drawn in Section VI.

Notations: In this paper, upper-case bold characters represent matrices, and lower-case bold characters represents vectors. $(\cdot)^T$, $(\cdot)^*$ and $(\cdot)^H$, respectively, stand for the transpose, conjugation and conjugate transpose of a matrix or vector. $E\{\cdot\}$ is the statistical expectation operator. $diag\{\mathbf{p}\}$ generates a diagonal matrix, whose diagonal elements are given by \mathbf{p} . $vec(\cdot)$ denotes the vectorization operator that turns a matrix into a vector by stacking all columns on top of the other, and \odot denotes the Khatri-Rao product. $\lceil b \rceil$ returns the smallest integer larger than b . $\|\cdot\|_F$ denotes the Frobenius norm. For two given sets of integers \mathbb{P}_1 and \mathbb{P}_2 , $\text{diff}(\mathbb{P}_1, \mathbb{P}_2) = \{\rho_1 - \rho_2 | \forall \rho_1 \in \mathbb{P}_1, \rho_2 \in \mathbb{P}_2\}$ is the set of cross differences of \mathbb{P}_1 with \mathbb{P}_2 .

II. PRELIMINARIES FOR SPARSE ARRAY

A. Difference Co-Array Generation Model

Assume that there are K far-field uncorrelated sources with incident angles of $\theta_1, \theta_2, \dots, \theta_K$, which are received by a sparse array of N elements with array positions of $\mathbb{P} = \{p_1, p_2, \dots, p_N\}d$, and unit spacing $d = \frac{\lambda}{2}$, where λ is the wavelength of the incident signal. Then, the received array data model at the time instant t is given by

$$\mathbf{x}(t) = \mathbf{A}\mathbf{s}(t) + \mathbf{n}(t), \quad (1)$$

where $\mathbf{A} = [\mathbf{a}(\theta_1), \mathbf{a}(\theta_2), \dots, \mathbf{a}(\theta_K)]$ is the $N \times K$ array steering matrix, whose columns are steering vectors in the form of $\mathbf{a}(\theta_k) = [e^{j\pi p_1 \sin(\theta_k)}, e^{j\pi p_2 \sin(\theta_k)}, \dots, e^{j\pi p_N \sin(\theta_k)}]^T$. $\mathbf{s}(t) = [s_1(t), \dots, s_K(t)]^T$ is the source signal vector and $\mathbf{n}(t)$ the noise vector. The covariance matrix is given by

$$\mathbf{R}_x = E[\mathbf{x}(t)\mathbf{x}^H(t)] = \mathbf{A}\mathbf{R}_s\mathbf{A}^H + \sigma_n^2\mathbf{I}_N, \quad (2)$$

where $\mathbf{R}_s = E[\mathbf{s}(t)\mathbf{s}^H(t)] = diag\{\mathbf{p}\}$, and $\mathbf{p} = [\delta_1^2, \delta_2^2, \dots, \delta_K^2]$ with δ_k^2 representing the power of the k -th source.

Then, vectorizing \mathbf{R}_x yields the following virtual array model:

$$\mathbf{z}_{\mathbb{P}} = \text{vec}(\mathbf{R}_x) = (\mathbf{A}^* \odot \mathbf{A})\mathbf{p} + \sigma_n^2\mathbf{1}_N, \quad (3)$$

where $\mathbf{1}_N = \text{vec}(\mathbf{I}_N)$, and $\mathbf{A}^* \odot \mathbf{A}$ is the steering matrix for the virtual array \mathbb{D} , whose sensor locations are obtained explicitly as:

$$\mathbb{D} = \{p_i - p_j | p_i, p_j \in \mathbb{P}\}. \quad (4)$$

The virtual array \mathbb{D} is also called the virtual co-array of the original array \mathbb{P} . As compared to (1), the vector $\mathbf{z}_{\mathbb{P}}$ in (3) can be considered as a single snapshot of the virtual array \mathbb{D} , whose observations behave like the data from the coherent source signal vector \mathbf{p} .

After removing the repetitive elements in the co-array, from which the longest possible continuous segment of \mathbb{D} , namely $\mathbb{U} = [-L_u, L_u]$, is selected, the corresponding measurements can be rearranged to form a new $(2L_u + 1) \times 1$ vector $\mathbf{z}_{\mathbb{U}}$ expressed as:

$$\mathbf{z}_{\mathbb{U}} = \mathbf{J}\mathbf{z}_{\mathbb{P}} = \mathbf{B}\mathbf{p} + \sigma_n^2 \mathbf{1}'_n, \quad (5)$$

where \mathbf{B} denotes the manifold matrix of the virtual ULA with dimension $(2L_u + 1) \times K$, $\mathbf{1}'_n = [\mathbf{0}_{1 \times L_u} \quad 1 \quad \mathbf{0}_{1 \times L_u}]^T$, and \mathbf{J} denotes a selection matrix of $(2L_u + 1) \times N^2$, where each row contains one non-zero element with its position corresponding to the index of the virtual element selected among the N^2 virtual sensors. Based on (5), underdetermined DOA estimation can be achieved using traditional subspace-based algorithms such as MUSIC and TLS-ESPRIT together with the spatial smoothing (SS) scheme [32], [33]. Besides, sparse representation based methods like LASSO [3] can also be used for DOA estimation, with higher estimation accuracy as well as higher computational complexity.

B. Mutual Coupling Model

The model in (1) does not consider MC between the physical sensors, which in practice can not be ignored, especially between sensors with small separations. Incorporating a coupling matrix \mathbf{C} to the observation, Eq. (1) can be modified as

$$\mathbf{x}(t) = \mathbf{C}\mathbf{A}\mathbf{s}(t) + \mathbf{n}(t), \quad (6)$$

where \mathbf{C} is determined by a variety of factors such as operating frequency, antenna type, sensor spacing, etc., which lead to a complicated expression for \mathbf{C} . In this paper, only the linear array geometry is of interest, and the MC effect is mainly determined by sensor spacing, and according to [34]–[37], \mathbf{C} can be expressed as

$$\mathbf{C}_{i,j} = \begin{cases} c_{|a_i - a_j|} & |a_i - a_j| \leq B, \\ 0 & |a_i - a_j| \geq B, \end{cases} \quad (7)$$

where the magnitude of $c_{|a_i - a_j|}$ is inversely proportional to the sensor spacing $|a_i - a_j|$, satisfying $1 = c_0 > |c_1| > |c_2| > \dots > |c_B| > |c_{B+1}| = 0$. Here, the MC coefficients in [37] are adopted as follows $c_l = c_1 e^{-j(l-1)/8}$, $2 \leq l \leq B$, and thus \mathbf{C} is completely determined by c_1 and sensor spacing. The larger c_1 is, the greater the coupling magnitude. For a given NLA, the level of total MC can be evaluated by the coupling leakage $L(N)$ [20] defined as:

$$L(N) = \frac{\|\mathbf{C} - \tilde{\mathbf{C}}\|_F}{\|\mathbf{C}\|_F}, \quad (8)$$

where

$$\tilde{\mathbf{C}}_{i,j} = \begin{cases} \mathbf{C}_{i,j}, & i = j \\ 0, & i \neq j \end{cases} \quad (9)$$

and $\|\mathbf{C} - \tilde{\mathbf{C}}\|_F$ is the energy of all non-diagonal components, characterizing the amount of MC. $L(N)$ is also called the energy ratio between two components, and theoretically, the larger $L(N)$ is, the greater the MC is.

In addition, the weight function $w(l)$ of a physical array \mathbb{P} is defined as the number of sensor pairs in \mathbb{P} that engender the co-array index l , that is,

$$w(l) = |\{(n_1, n_2) \in \mathbb{P}^2 | n_1 - n_2 = l\}|, l \in \mathbb{D}. \quad (10)$$

The notation \mathbb{P}^2 indicates that both elements n_1 and n_2 are selected from the set \mathbb{P} .

The weight function $w(l)$ of any linear array with N sensors has the following properties [34]

$$w(0) = N, \sum_{l \in \mathbb{D}} w(l) = N^2, w(l) = w(-l). \quad (11)$$

III. THE STRATEGY OF MULTI-SUBARRAY DILATED NESTED ARRAY (MDNA)

In this section, we present a systematic design named MDNA, which expands the sparse subarrays of nested arrays to increase the virtual aperture, and lays the foundation for the introduction of the AMDNA in the subsequent section.

A. Introduction to NA

A nested array consists of a dense ULA (ULA0) spaced $d = \frac{\lambda}{2}$ with N_1 elements, and a sparse ULA (ULA1) of N_2 elements with spacing $(N_1 + 1)d$. It has been demonstrated that the cross-difference between ULA1 and ULA0 leads to a virtual co-array without holes. The holes in the sparse ULA1 are filled by the virtual elements generated from the cross-difference to ULA0, which can be considered as virtual migration of ULA0 by $N_1 d$ to form a hole-free virtual array.

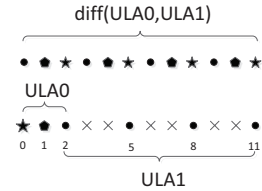


Fig. 1: An NA example and its DCA with $N_1 = N_2 = 3$.

For example, Fig. 1 shows an NA with $N_1 = N_2 = 3$. By calculating the difference between the element labeled 5 in ULA1 and all the elements in ULA0, the virtual array elements $\{3, 4, 5\}$ in ULA1 are obtained, which can be regarded as the virtual array elements obtained by shifting ULA0 to the right by a distance of $3d$, and then filling the holes between elements labeled 2 and 5. The same procedure can be performed to fill the remaining holes in ULA1 by shifting ULA0 by an appropriate distance.

B. Proposed MDNA Scheme

Inspired by the idea of virtual migration of a dense ULA0 in NA, a novel systematic strategy called MDNA is designed by firstly sparsifying the ULA0 in NA into a new array named ULA(0) with spacing Dd and N_1 elements, and starting from the element labeled 0. Further, in order to obtain a DCA without holes, each element of ULA1 in NA is changed into several ULAs named from ULA(1) to ULA(X), and each sub-ULA is spaced by $d = \frac{\lambda}{2}$ and the number of elements is D .

This result motivates the multi-subarray dilated nested array (MDNA) scheme, as described below.

Definition 1: The MDNA can be represented by N_1, X, D , defined as:

$$\mathbb{S} = \bigcup_{i=0,1,\dots,X} \text{ULA}(i), \quad (12)$$

where

$$\text{ULA}(0) = \{0, D, \dots, (N_1 - 1)D\}, \quad (13)$$

$$\text{ULA}(1) = \{0, -1, \dots, -(D - 1)\}, \quad (14)$$

$$\text{ULA}(X) = \text{ULA}(X - 1) - (N_1 D + D - 1), (X \geq 2). \quad (15)$$

Obviously, the difference between ULA(0) and ULA(1) can form a hole-free virtual ULA $[0, N_1 D - 1]$, denoted as \mathbb{S}_1 . For example, in Fig. 2, with $D = 3$, $N_1 = 4$, the virtual array elements are obtained from the cross-difference between ULA(0) and ULA(1), which can be considered as the case that ULA(0) is shifted right by d and $2d$, respectively; thus, it is able to fill all the holes in ULA(0) exactly, forming a virtual DCA without holes. Furthermore, we can adjust the spacing of ULA(1) and ULA(2) as $N_1 D + D - 1$. In the same way, the cross-difference between ULA(0) and ULA(2) can form a hole-free virtual ULA $[N_1 D + D - 1, 2N_1 D + D - 2]$, denoted as \mathbb{S}_2 . It can be seen that the result of \mathbb{S}_2 is right shifted by $N_1 D + D - 1$ from \mathbb{S}_1 , but unfortunately \mathbb{S}_1 and \mathbb{S}_2 are not seamlessly connected. In order to fill the holes between \mathbb{S}_1 and \mathbb{S}_2 , the cross-difference between ULA(1) and ULA(2) can be exploited. Similar procedures can be followed for the cross-difference between ULA(X) and ULA(0), along with the cross-difference between ULA(X) and ULA(1), where the maximum number of DOFs is larger than the parent NA. It can be seen that the structural design of MNA is limited by the total number of array elements, i.e. $N_1 + N_2 = N$, where $N_2 = DX - 1$, D and X are arbitrary positive integers. Compared to NA, MDNA increases the number of DOFs by selecting the appropriate spacing among the subarrays ULA(1), ULA(2), ..., ULA(X), while maintaining the hole-free DCA with the following two properties:

Property 1: The DCA of MDNA is hole-free and has a maximum virtual array aperture of $L = N_1 X D + DX - D - X$.

Proof: Firstly, the DCA between ULA(0) and ULA(1) (due to symmetry of the DCA, only positive part is considered here) is given by:

$$\text{diff}[\text{ULA}(0), \text{ULA}(1)] = [0, N_1 D - 1]. \quad (16)$$

Similarly, we have

$$\begin{aligned} \text{diff}[\text{ULA}(0), \text{ULA}(x)] &= \text{diff}[\text{ULA}(0), \text{ULA}(1)] \\ &+ (x - 1)(N_1 D + D - 1) \\ &= [0, N_1 D - 1] + (x - 1)(N_1 D + D - 1) \end{aligned} \quad (17)$$

$$\begin{aligned} \text{diff}[\text{ULA}(1), \text{ULA}(x)] &= \text{diff}[\text{ULA}(1), \text{ULA}(1)] \\ &+ (x - 1)(N_1 D + D - 1) \\ &= [-(D - 1), D - 1] + (x - 1)(N_1 D + D - 1) \end{aligned} \quad (18)$$

$$\begin{aligned} \text{diff}[\text{ULA}(0), \text{ULA}(x + 1)] &= \text{diff}[\text{ULA}(0), \text{ULA}(1)] \\ &+ x(N_1 D + D - 1) \\ &= [0, N_1 D - 1] + x(N_1 D + D - 1) \\ \text{diff}[\text{ULA}(1), \text{ULA}(x + 1)] &= \text{diff}[\text{ULA}(1), \text{ULA}(1)] \\ &+ x(N_1 D + D - 1) \\ &= [-(D - 1), D - 1] + x(N_1 D + D - 1). \end{aligned} \quad (19)$$

Combining Eqs. (17) and (18), the consecutive range for the DCA of the proposed MDNA set is obtained as $L_x = [-(D - 1), N_1 D - 1] + (x - 1)(N_1 D + D - 1)$; similarly, the DCA set $L_{x+1} = [-(D - 1), N_1 D - 1] + x(N_1 D + D - 1)$ is obtained with Eqs. (19) and (20). It can be readily seen that the minimum of L_{x+1} is

$$\begin{aligned} &x(N_1 D + D - 1) - (D - 1) \\ &= xN_1 D + (x - 1)(D - 1), \end{aligned} \quad (21)$$

while the maximum of L_x is

$$\begin{aligned} &(x - 1)(N_1 D + D - 1) + N_1 D - 1 \\ &= xN_1 D + (x - 1)(D - 1) - 1, \end{aligned} \quad (22)$$

where $x = 1, \dots, X - 1$. Obviously, when $X \geq 2$, L_x and L_{x+1} are seamlessly connected to each other proving that the DCA of MDNA is hole-free. The maximum aperture can be calculated directly from the largest distance of virtual DCA, whose rightmost end is $D(N_1 - 1)$ and the leftmost end is $-(D - 1) - (X - 1)(N_1 D + D - 1)$. Therefore, the DCA's maximum continuous segment of MDNA on one side is:

$$\begin{aligned} L &= D(N_1 - 1) + [(D - 1) + (X - 1)(N_1 D + D - 1)] \\ &= N_1 X D + DX - D - X. \end{aligned} \quad (23)$$

This completes the proof.

Property 2: If $D > 1, X > 1$, the number of DOFs of MDNA is higher than that of NA, and if $D = 1$ or $X = 1$, MDNA and NA have the same number of DOFs.

Proof: The number of DOFs of MDNA is derived for a given fixed total number of sensors N as shown in Eq. (24), and the optimal closed-form expression for three parameters N, D and X is introduced to achieve the highest number of DOFs of MDNA as follows

$$N = N_1 + N_2 = N_1 + DX - 1. \quad (24)$$

Substituting Eq. (24) into Eq. (23), we have

$$L = (N_1 + 1)(N + 1 - N_1) - D - X. \quad (25)$$

Then, Eq. (25) is solved with respect to variable N_1 by taking the partial derivative of L , while keeping D and X as a constant, which gives the following result

$$L'_{N_1} = N - 2N_1. \quad (26)$$

In the following, two cases are considered with N being even and odd, respectively. When N is even, from Eq. (26), the largest number of DOFs can be obtained with $N_1 = \frac{N}{2}$, and thus, we have $N_2 = DX - 1 = \frac{N}{2}$. By substituting $N_1 = \frac{N}{2}$ into Eq. (25), we have:

$$\begin{aligned} L &= \left(\frac{N}{2} + 1\right)(N + 1 - \frac{N}{2}) - D - X \\ &= \frac{N^2}{4} + N + 1 - (D + X). \end{aligned} \quad (27)$$

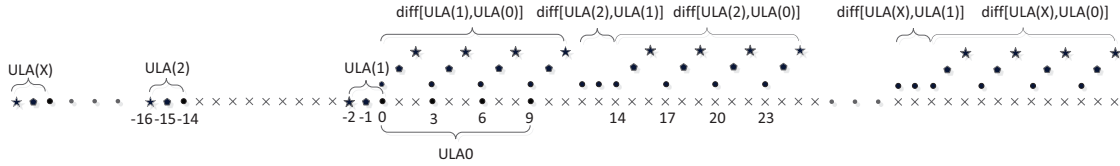


Fig. 2: An MDNA example and its DCA with $D = 3$ and $N_1 = 4$.

Therefore, the maximum aperture L is determined by D and X with fixed N_1 . In the case of $DX = \frac{N}{2} + 1$, it is obvious that the longest L can be obtained when $D = X = \sqrt{\frac{N}{2} + 1}$. Since both D and X need to be integers, it is not always possible to obtain the theoretically optimum integer value, and thus, the closest possible integers D and X should be chosen, which in turn should reconsider the value of N_1 to be $N_1 = \lceil \frac{N}{2} \rceil + 1$.

Note that if DX is a prime number, only $D = 1$ or $X = 1$ can be chosen, leading to the maximum value $D + X = 2 + \frac{N}{2}$. By substituting the maximum value $D + X$ into Eq. (27), the theoretical minimum value for the maximum aperture of MDNA is calculated as follows

$$L_{\min} = \frac{N^2}{4} + \frac{N}{2} - 1, \quad (28)$$

whose corresponding number of DOFs is:

$$\text{DOF} = 2L + 1 = \frac{N^2}{2} + N - 1. \quad (29)$$

Compared to the DOF achieved by NA with the same total number of array elements N , it can be shown that $L_{\min} = L_{\text{nest}}$ (L_{nest} is the maximum aperture of the NA). Thus, it can be concluded that the number of DOFs of MDNA is greater than NA under the condition that neither D nor X equals 1.

When N is odd, we have $N_1 = \frac{N+1}{2}$ and $N_2 = \frac{N-1}{2}$, which are substituted into Eq. (25) as follows

$$\begin{aligned} L &= \left(\frac{N+1}{2} + 1\right) \left(\frac{N-1}{2} + 1\right) - D - X \\ &= \frac{N^2}{4} + N + \frac{3}{4} - (D + X). \end{aligned} \quad (30)$$

Thus, we get $DX = \frac{N-1}{2} + 1 = \frac{N+1}{2}$. Similarly, when $D = 1$ or $X = 1$, $D + X$ reaches the maximum value:

$$D + X = \frac{N + 3}{2}. \quad (31)$$

Substituting (31) into Eq. (30), we obtain:

$$L_{\min} = \frac{N^2}{4} + \frac{N}{2} - \frac{3}{4}, \quad (32)$$

whose corresponding number of DOFs is

$$\text{DOF} = 2L + 1 = \frac{N^2}{2} + N - \frac{1}{2}. \quad (33)$$

The same conclusion for MDNA in comparison with NA can be drawn for the even case. This completes the proof.

C. Relationship with NA

From *property 2*, it can be seen that MDNA has the same number of DOFs as NA in the case of $D = 1$ or $X = 1$, where the structure of MDNA is reduced into NA, and thus NA can be treated as a special case of MDNA.

For $X = 1$, MDNA only has two ULAs: $\text{ULA}(0) = \{0, D, \dots, (N_1 - 1)D\}d$ and $\text{ULA}(1) = \{0, -1, \dots, -(D-1)\}d$. It can be seen that $\text{ULA}(1)$ is exactly the dense ULA with number D and spacing d in the NA, and $\text{ULA}(0)$ is the sparse ULA with number N_1 and spacing Dd in the NA. When $D = 1$, the $\text{ULA}(0)$ of MDNA is equivalent to the dense ULA in NA, whose sparse ULA is formed with the sub-ULAs from $\text{ULA}(1)$ to $\text{ULA}(X)$ of MDNA. Fig. 3 shows the two special cases of MDNA, when $D = 1, X = 3, N_1 = 4$ and $D = 3, X = 1, N_1 = 4$ respectively. In Fig. 3 (a), MDNA is consistent with NA, while in Fig. 3 (b), MDNA is a mirrored NA.

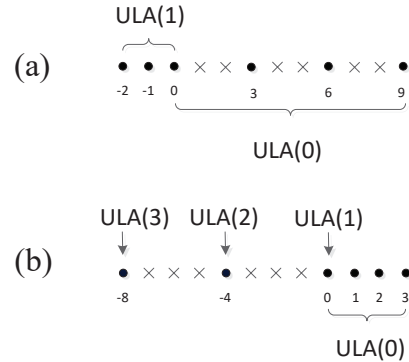


Fig. 3: Two special cases of MDNA: (a) $D = 3, X = 1$ (b) $D = 1, X = 3$.

IV. THE PROPOSED AMDNA

The proposed MDNA earlier n has more DOFs than NA and less MC through the expansion of multi-subarray. Yet there are still dense multiple sub-ULAs in the proposed MDNA. In this section, an augmented MDNA (AMDNA) is proposed by migrating some of the dense elements in MDNA, which further reduces the MC while still maintaining a reasonable number of DOFs. The specific form of the AMDNA is given as follows:

Definition 2: (Augmented multi-subarray dilated nested array) AMDNA can be represented by N_1, X, D , defined as:

$$\mathcal{S}' = \bigcup_{i=0,1,\dots,X} \text{ULA}(i) \quad (34)$$

$$\text{ULA}(0) = \{0, D, \dots, (N_1 - 1)D\} \quad (35)$$

$$\text{ULA}(x) = \text{ULA}(x.1) \cup \text{ULA}(x.2), x = 1, 2, \dots, X. \quad (36)$$

If D is odd: where if x is odd,

$$\text{ULA}(x.1) = \{(1-x)(N_1D + D - 1) - 2l_1 \mid 0 \leq l_1 \leq \frac{D-1}{2}\} \quad (37)$$

$$\text{ULA}(x.2) = \{(x-1)(N_1D + D - 1) + (N_1 - 1)D + 1 + 2l_2 \mid 0 \leq l_2 \leq \frac{D-3}{2}\}, \quad (38)$$

if x is even,

$$\text{ULA}(x.1) = \{(1-x)(N_1D + D - 1) - 2l_2 - 1 \mid 0 \leq l_2 \leq \frac{D-3}{2}\} \quad (39)$$

$$\text{ULA}(x.2) = \{(x-1)(N_1D + D - 1) + (N_1 - 1)D + 2l_1 \mid 0 \leq l_1 \leq \frac{D-1}{2}\}. \quad (40)$$

If D is even: where if x is odd,

$$\text{ULA}(x.1) = \{(1-x)(N_1D + D - 1) - 2l_1 \mid 0 \leq l_1 \leq \frac{D-2}{2}\} \quad (41)$$

$$\text{ULA}(x.2) = \{(x-1)(N_1D + D - 1) + (N_1 - 1)D + 1 + 2l_2 \mid 0 \leq l_2 \leq \frac{D-2}{2}\} \quad (42)$$

if x is even,

$$\text{ULA}(x.1) = \{(1-x)(N_1D + D - 1) - 2l_2 - 1 \mid 0 \leq l_2 \leq \frac{D-2}{2}\} \quad (43)$$

$$\text{ULA}(x.2) = \{(x-1)(N_1D + D - 1) + (N_1 - 1)D + 2l_1 \mid 0 \leq l_1 \leq \frac{D-2}{2}\}. \quad (44)$$

Comparing Eqs. (14) and (15) in *Definition 1* with Eq. (36) in *Definition 2*, it can be seen that AMDNA is designed by removing some elements of the dense sub-ULAs in MDNA, so that the MC level can be reduced. To minimize the MC, considering the MDNA, the elements in $\text{ULA}(x) = \{(1-x)(N_1D + D - 1) - l \mid 0 \leq l \leq D - 1\}$ are divided into odd parts and even parts, named $\text{ULA}(x.a)$ and $\text{ULA}(x.b)$, respectively.

When D is odd,

$$\text{ULA}(x.a) = \{(1-x)(N_1D + D - 1) - 2l \mid 0 \leq l \leq \frac{D-1}{2}\}, \quad (45)$$

$$\text{ULA}(x.b) = \{(1-x)(N_1D + D - 1) - 2l - 1 \mid 0 \leq l \leq \frac{D-3}{2}\}. \quad (46)$$

and when D is even,

$$\text{ULA}(x.a) = \{(1-x)(N_1D + D - 1) - 2l \mid 0 \leq l \leq \frac{D-2}{2}\}, \quad (47)$$

$$\text{ULA}(x.b) = \{(1-x)(N_1D + D - 1) - 1 - 2l \mid 0 \leq l \leq \frac{D-2}{2}\}. \quad (48)$$

Then, the corresponding $\text{ULA}(x.a)$ or $\text{ULA}(x.b)$ is selected to migrate symmetrically related to $\text{ULA}(0)$ according to the parity of x . When x is even, the elements in $\text{ULA}(x.a)$

migrates symmetrically with respect to $\text{ULA}(0)$, and if x is odd, the elements in $\text{ULA}(x.b)$ migrates symmetrically with respect to $\text{ULA}(0)$. As a result, the new position of the moved element constitutes $\text{ULA}(x.2)$ in AMDNA, and the elements in $\text{ULA}(x.1)$ are the remaining unmoved elements. Each moved element in AMDNA and its original position in MDNA are symmetrical with respect to $\text{ULA}(0)$. For example, in Fig. 4, we show how the AMDNA with $D = X = 3, N_1 = 5$ evolves from MDNA. Specifically for MDNA, $\text{ULA}(1.a) = \{0, -2\}$, $\text{ULA}(1.b) = \{-1\}$, $\text{ULA}(2.a) = \{-17, -19\}$, $\text{ULA}(2.b) = \{-18\}$, $\text{ULA}(3.a) = \{-34, -36\}$, $\text{ULA}(3.b) = \{-35\}$. Therefore, the elements in $\text{ULA}(1.a)$, $\text{ULA}(2.b)$ and $\text{ULA}(3.a)$ are migrated symmetrically with respect to $\text{ULA}(0)$, which correspondingly constitute $\text{ULA}(1.2)$, $\text{ULA}(2.2)$ and $\text{ULA}(3.2)$ in AMDNA, respectively..

After the above-mentioned migration, the DOFs of the proposed AMDNA can be maintained as compared to MDNA, while the MC is greatly reduced. Two properties of the proposed AMDNA are given as follows.

Property 3: The number of one-side uniform DOFs of the proposed AMDNA is $L = N_1XD + DX - D - X$ when the parity of D and X is different, and $L = N_1XD + DX - D - X + 1$ if parity is the same.

Proof: It can be seen that since the element in $\text{ULA}(x.2)$ of AMDNA and its original position in MDNA are symmetrical with respect to $\text{ULA}(0)$, the cross-difference between $\text{ULA}(x.1)$ and $\text{ULA}(0)$ as well as $\text{ULA}(x.2)$ and $\text{ULA}(0)$ in AMDNA is equivalent to the cross-difference between $\text{ULA}(x)$ and $\text{ULA}(0)$ in MDNA, i.e.

$$\begin{aligned} & \text{diff}(\text{ULA}(x), \text{ULA}(0)) \\ &= \text{diff}(\text{ULA}(x.1), \text{ULA}(0)) \cup \text{diff}(\text{ULA}(x.2), \text{ULA}(0)). \end{aligned} \quad (49)$$

Therefore, the DCA of AMDNA is given by:

$$\begin{aligned} & \bigcup_{i=1}^X \text{diff}(\text{ULA}(i), \text{ULA}(0)) \\ &= \{(i-1)(N_1D + D - 1) + l \mid 0 \leq l \leq N_1D - 11 \leq i \leq X\}. \end{aligned} \quad (50)$$

From Eq. (50), it can be seen that there are some holes defined as:

$$\{i(N_1D + D - 1) + l \mid l \in \mathbb{V}, 0 \leq i \leq X - 2\}, \quad (51)$$

where $\mathbb{V} = [N_1D, N_1D + D - 2]$.

Next, we show that the cross-difference between sub-ULAs of AMDNA, namely $\text{ULA}(x)$ in Eq. (34), can completely fill the holes in Eq. (51) (only the positive half of the DCA is considered).

When D is odd: if x is odd, where $x \geq 3$, we have

$$\begin{aligned} & \text{diff}(\text{ULA}(x.1), \text{ULA}(1.1)) \\ &= \{l + (x-2)(N_1D + D - 1) \mid l \in \mathbb{V}_{11}\} \end{aligned} \quad (52)$$

$$\begin{aligned} & \text{diff}(\text{ULA}((x-1).2), \text{ULA}(1.1)) \\ &= \{l + (x-2)(N_1D + D - 1) \mid l \in \mathbb{V}_{12}\}, \end{aligned} \quad (53)$$

where $\mathbb{V}_{11} = \{N_1D, N_1D + 2, \dots, N_1D + 2D - 2\}$ and $\mathbb{V}_{12} = \{N_1D - D, N_1D - D + 2, \dots, N_1D + D - 2\}$.

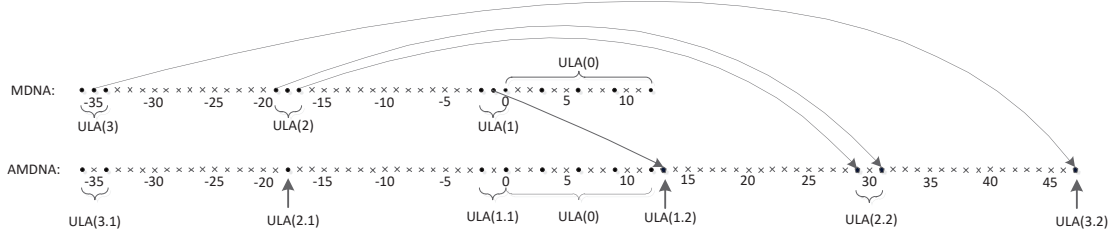


Fig. 4: An example for the change from MDNA to AMDNA with $N_1 = 5$, $D = 3$ and $X = 3$.

It should be noted that (52) and (53) both have a numerical span of 2. Since D is an odd number, the parity of (52) and (53) is different. By combining (52) and (53), we can extrapolate:

$$\begin{aligned} & \text{diff}(\text{ULA}((x-1).2), \text{ULA}(1.1)) \cup \\ & \text{diff}(\text{ULA}(x.1), \text{ULA}(1.1)) \\ & \supseteq \{l + (x-2)(N_1D + D - 1) \mid l \in \mathbb{V}\}, \end{aligned} \quad (54)$$

if x is even, where $x \geq 2$,

$$\begin{aligned} & \text{diff}(\text{ULA}(1.1), \text{ULA}(x.1)) \\ & = \{l + (x-2)(N_1D + D - 1) \mid l \in \mathbb{V}_{21}\} \end{aligned} \quad (55)$$

$$\begin{aligned} & \text{diff}(\text{ULA}(1.2), \text{ULA}((x-1).1)) \\ & = \{l + (x-2)(N_1D + D - 1) \mid l \in \mathbb{V}_{22}\}, \end{aligned} \quad (56)$$

where $\mathbb{V}_{21} = \{N_1D + 1, N_1D + 3, \dots, N_1D + 2D - 3\}$ and $\mathbb{V}_{22} = \{N_1D - D + 1, N_1D - D + 3, \dots, N_1D + D - 3\}$.

Combining Eqs. (55) and (56), we obtain

$$\begin{aligned} & \text{diff}(\text{ULA}(1.1), \text{ULA}(x.1)) \cup \\ & \text{diff}(\text{ULA}(1.2), \text{ULA}((x-1).1)) \\ & \supseteq \{l + (x-2)(N_1D + D - 1) \mid l \in \mathbb{V}\}. \end{aligned} \quad (57)$$

It can be known from Eqs. (54) and (57) that for $x = 2, 3, \dots, X$, the holes described in (51) can be filled. Therefore, when D is odd, the maximum number of DOFs is the same as the MDNA.

Similarly, when D is even: if x is odd, where $x \geq 3$,

$$\begin{aligned} & \text{diff}(\text{ULA}(1.2), \text{ULA}((x-1).1)) \\ & = \{l + (x-2)(N_1D + D - 1) \mid l \in \mathbb{V}_{31}\} \end{aligned} \quad (58)$$

$$\begin{aligned} & \text{diff}(\text{ULA}(1.1), \text{ULA}(x.1)) \\ & = \{l + (x-2)(N_1D + D - 1) \mid l \in \mathbb{V}_{32}\}, \end{aligned} \quad (59)$$

where $\mathbb{V}_{31} = \{N_1D - D + 2, N_1D - D + 4, \dots, N_1D + D - 2\}$ and $\mathbb{V}_{32} = \{N_1D + 1, N_1D + 3, \dots, N_1D + 2D - 3\}$.

Combining Eqs. (58) and (59), we obtain,

$$\begin{aligned} & \text{diff}(\text{ULA}(1.2), \text{ULA}((x-1).1)) \cup \\ & \text{diff}(\text{ULA}(1.1), \text{ULA}(x.1)) \\ & \supseteq \{l + (x-2)(N_1D + D - 1) \mid l \in \mathbb{V}\}, \end{aligned} \quad (60)$$

if x is even, where $x \geq 2$,

$$\begin{aligned} & \text{diff}(\text{ULA}(1.1), \text{ULA}(x.1)) \cup \text{diff}(\text{ULA}(x.2), \text{ULA}(1.2)) \\ & \supseteq \{l + (x-2)(N_1D + D - 1) \mid l \in \mathbb{V}_{41}\} \end{aligned} \quad (61)$$

$$\begin{aligned} & \text{diff}(\text{ULA}((x-1).2), \text{ULA}(1.1)) \\ & \supseteq \{l + (x-2)(N_1D + D - 1) \mid l \in \mathbb{V}_{42}\}, \end{aligned} \quad (62)$$

where $\mathbb{V}_{41} = \{N_1D, N_1D + 2, \dots, N_1D + 2D - 2\}$ and $\mathbb{V}_{42} = \{N_1D - D + 1, N_1D - D + 3, \dots, N_1D + D - 3\}$.

Combining Eqs. (61) and (62) leads to

$$\begin{aligned} & \text{diff}(\text{ULA}(1.1), \text{ULA}(x.1)) \cup \text{diff}(\text{ULA}(x.2), \text{ULA}(1.2)) \\ & \cup \text{diff}(\text{ULA}((x-1).2), \text{ULA}(1.1)) \\ & \supseteq \{l + (x-2)(N_1D + D - 1) \mid l \in \mathbb{V}\}. \end{aligned} \quad (63)$$

Therefore, when D is even, the maximum number of DOFs is also the same as the MDNA. Specifically, when D and X have the same parity, the leftmost element of AMDNA is labeled by $-(D-1) - (X-1)(N_1D + D - 1)$, and its DCA with the $(N_1-1)D + 1$ element in ULA(1.2) yields the virtual element labeled by $N_1DX + DX - D - X + 1$.

This completes the proof.

Next, to show the difference in uDOFs of the MDNA and AMDNA along with other considered sparse arrays, we list the number of uDOFs of nine types of arrays for comparison in Table I. It should be noted that when the number of sensors is less than 13 in the table, there is no corresponding configurations for ePCA and TS-ENA. When the number of sensors is larger than 13, it is observed that ePCA has the least number of uDOFs among all arrays, while TS-ENA offers the maximum number. In addition, it can be seen that MDNA and AMDNA provide a higher number of uDOFs than the NA, 2-SNA and D-DNA, but a less number than the MISC, ANAI-2 and TS-ENA.

It is well-known that the weight functions at small separations of sensor pairs are of great importance for MC evaluation [20]. Especially, the first three weight functions, $w(1)$, $w(2)$ and $w(3)$ have a dominated impact on the MC of a physical array. Therefore, the first three weight functions of AMDNA are given in *Property 4* to evaluate the MC level.

Property 4: The weight function $w(m)$ of AMDNA at $m = 1, 2, 3$, with the required condition $D \geq 2$, $N_1 \geq 2$, is given as follows:

$$\begin{aligned} w(1) &= 1, \\ w(2) &= \begin{cases} (D-2) * X, & \text{if } D > 2, \\ N_1 - 1, & \text{if } D = 2, \end{cases} \\ w(3) &= \begin{cases} 1, & \text{if } D \neq 3, \\ N_1 - 1, & \text{if } D = 3. \end{cases} \end{aligned} \quad (64)$$

Proof: AMDNA can be divided into $X+1$ ULAs, as shown by (34). For the DCA of \mathbb{S}' , obviously, it can be achieved as

TABLE I: A summary of uDOFs of nine types of arrays for different number of sensors (N).

Sensors number	NA	2-SNA	MISC	D-DNA	ePCA	ANAI-2	MDNA	AMDNA	TS-ENA
9	49	49	59	49	/	53	51	51	/
17	161	161	187	161	157	173	169	171	203
21	241	241	275	241	217	257	247	247	293
28	419	419	467	421	359	443	435	437	489
31	511	511	563	513	445	537	529	531	589
35	647	647	707	649	541	677	667	667	735

TABLE II: A summary of weight functions and MC leakage of eight types of arrays.

Array config.	2-SNA	MISC	D-DNA	ePCA	ANAI-2	MDNA	AMDNA	TS-ENA
17 sensors	$N_1 = 8$		$N_1 = 8$	$M = 5$	$N_1 = 8$	$N_1 = 9$	$N_1 = 9$	$N_1 = 10$
	$N_2 = 9$	$N = 17$	$N_2 = 5$	$N_c = 8$	$N_2 = 9$	$D = 3$	$D = 3$	$N_2 = 6$
						$X = 3$	$X = 3$	
$w(1)$	2	1	1	1	2	6	1	4
$w(2)$	5	6	7	1	7	3	3	2
$w(3)$	4	1	1	1	2	8	8	1
L	0.2113	0.1848	0.1731	0.1462	0.2176	0.2827	0.1810	0.2267
28 sensors	$N_1 = 14$		$N_1 = 15$	$M = 8$	$N_1 = 14$	$N_1 = 14$	$N_1 = 14$	$N_1 = 10$
	$N_2 = 14$	$N = 28$	$N_2 = 7$	$N_c = 13$	$N_2 = 14$	$D = 3$	$D = 3$	$N_2 = 6$
						$X = 5$	$X = 5$	
$w(1)$	2	1	1	1	2	10	1	8
$w(2)$	11	12	11	1	12	5	5	6
$w(3)$	4	1	1	1	2	13	13	5
L	0.2027	0.1859	0.1760	0.1139	0.2007	0.2833	0.1688	0.2531
31 sensors	$N_1 = 15$		$N_1 = 16$	$M = 9$	$N_1 = 15$	$N_1 = 16$	$N_1 = 16$	$N_1 = 16$
	$N_2 = 16$	$N = 31$	$N_2 = 8$	$N_c = 14$	$N_2 = 16$	$D = 4$	$D = 4$	$N_2 = 14$
						$X = 4$	$X = 4$	
$w(1)$	1	1	1	1	2	12	1	10
$w(2)$	14	12	13	1	14	8	8	8
$w(3)$	1	1	1	1	2	4	1	7
L	0.1887	0.1773	0.1790	0.1056	0.2013	0.2916	0.1624	0.2700

follows

$$\text{DCA} = \sum_{i=0}^X \sum_{j=0}^X \text{diff}(\text{ULA}(i), \text{ULA}(j)), \quad (65)$$

which is the self-difference and cross-difference of sub-ULAs for the cases of $i = j$ and $i \neq j$. We mainly focus on the self-difference of sub-ULAs and the cross-difference between adjacent ULAs to calculate the first three weight functions of AMDNA.

Obviously, according to Definition 2, it can be seen that the inter-sensor spacing of ULA(0) is D , whose self-differences contain $\pm D, \pm 2D$, and so on. The inter-sensor spacing of the ULA(x .1) and ULA(x .2) is 2, whose self-differences include $\pm 2, \pm 4$, and so on. Thus, we can obtain

$$(D - 2) * X \quad (66)$$

sensor pairs with separation 2 and

$$(N_1 - 1) \quad (67)$$

sensor pairs with separation D .

Next, for the cross-differences between ULA(1.1) and ULA(x .1), along with ULA(1.2) and ULA(x .2), it can be

clearly seen from Definition 2, that the minimum inter-sensor spacing is greater than $N_1 D \geq 4$. Therefore, we only consider the cross-differences between ULA(1.1), ULA(1.2) and ULA(0) to calculate the first three weight functions. In Definition 2, ULA(0) and ULA(1.1) have a common sensor labeled 0; to facilitate analysis, it is considered as part of ULA(1.1), and we have

$$\min \text{diff}(\text{ULA}(1.1), \text{ULA}(0)) = D. \quad (68)$$

Furthermore, the first and second minimum elements of $\text{diff}(\text{ULA}(1.2), \text{ULA}(0))$ are given as follows:

$$\min_1 \text{diff}(\text{ULA}(1.2), \text{ULA}(0)) = N_1 D + 1 - N_1 D = 1. \quad (69)$$

When $D > 3$, we have

$$\min_2 \text{diff}(\text{ULA}(1.2), \text{ULA}(0)) = N_1 D + 3 - N_1 D = 3, \quad (70)$$

when $D = 2$, we have

$$\min_2 \text{diff}(\text{ULA}(1.2), \text{ULA}(0)) = N_1 D + 1 - (N_1 - 1) D = 3. \quad (71)$$

Therefore, according to (66) to (71), Property 4 is proved.

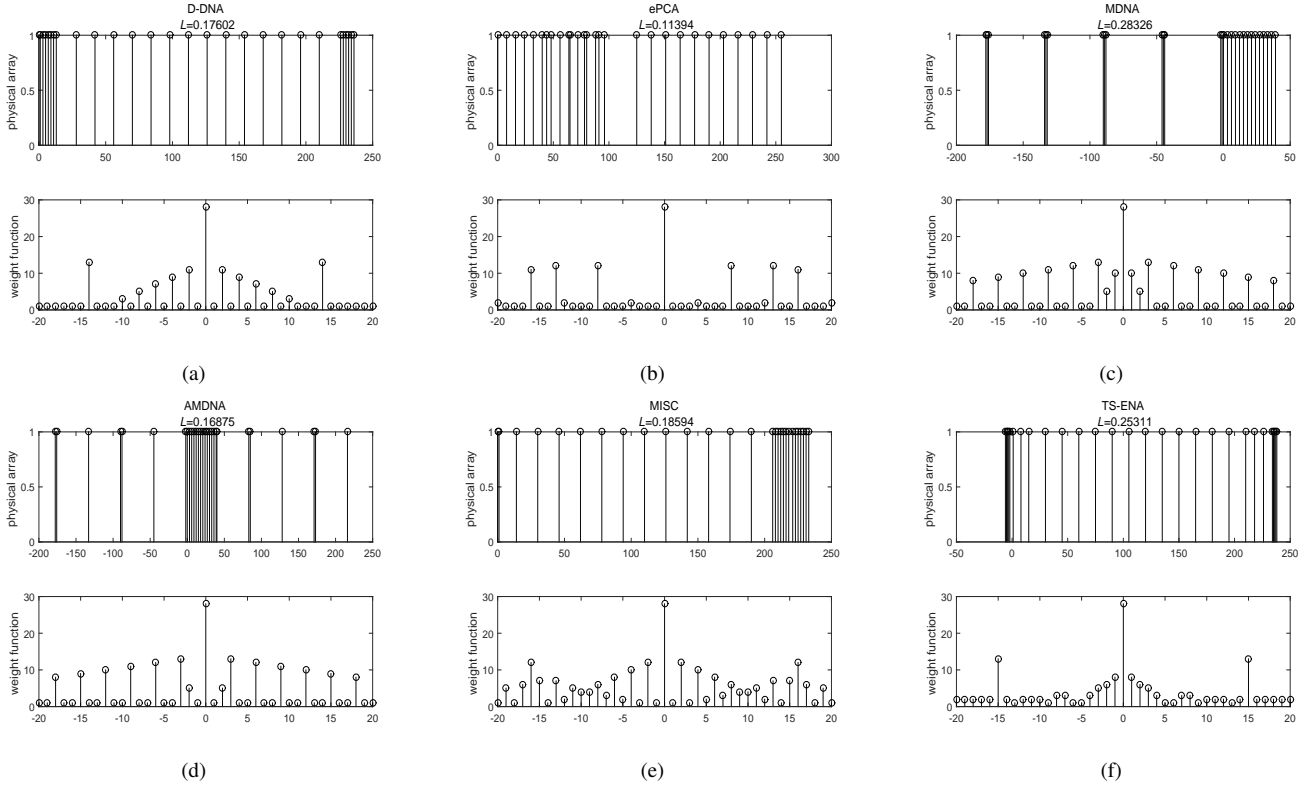


Fig. 5: The positions of the array elements and their weight functions where the number of sensors (N) is 2: (a) D-DNA, (b) ePCA, (c) MDNA, (d) AMDNA, (e) MISC, (f) TS-ENA.

V. SIMULATION RESULTS

As shown in Tables I and II, and also demonstrated in [29], the MISC array outperforms the NA [10], 2-SNA [20], ANAI-2 [22] in terms of both number of DOFs and mutual coupling, so we will only compare our proposed arrays with MISC, D-DNA [23], ePCA [27] and TS-ENA [19]. In this section, to demonstrate the performance of the proposed AMDNA, a comparison of the DOA estimation performance among all arrays is conducted with the sparse representation based method like LASSO [3], as well as SS-based subspace method like TLS-ESPRIT [22]. The estimation performance for different array configurations is evaluated in terms of the root mean square error (RMSE), defined as

$$\text{RMSE} = \sqrt{\frac{1}{1000K} \sum_{q=1}^{1000} \sum_{k=1}^K (\hat{\theta}_{k,q} - \theta_k)^2} \quad (72)$$

where θ_k represents the true DOA of the k -th source and $\hat{\theta}_{k,q}$ denotes the corresponding estimate obtained at the q -th trial. Similar to [20], the uniform DOFs, rather than the array aperture, is employed in the following to investigate the overall estimation performance.

A. Mutual Coupling Evaluated for Sparse Array

To illustrate the MC level of the above-mentioned six types of 28-sensor sparse arrays, the weight function and corresponding MC leakage are given in Fig. 5, along with

the position of physical sensors. A summary of the weight functions ($w(1)$, $w(2)$ and $w(3)$) and MC leakage (L) is provided in Table II. It can be seen that TS-ENA and MDNA produce a higher value of L than other arrays except that ePCA has the least value of L . According to the value of L , MISC, D-DNA and AMDNA are much less sensitive to the MC effect. As the number of sensors increases, more specifically when $N = 31$, the value of L of AMDNA is smaller than that of other arrays except for ePCA, implying that it experiences the least MC effect. Combined with Table I, it is clearly seen that the proposed AMDNA has achieved a good compromise in terms of uDOFs and MC leakage among arrays being considered, which will also be demonstrated in DOA estimation results next.

B. DOA Estimation in the Absence of Mutual Coupling

Note that, sparse representation based method can utilize all unique lags in the difference coarray, thus achieving better DOA estimation accuracy than the subspace based methods which can only utilize those continuous lags. However, as here we focus on the uniform DOFs, in the following simulations, we only use the continuous segment of DCA for sparse reconstruction.

In the absence of mutual coupling, the simulation parameters are set as follows: 27 sources uniformly distributed between -60° to 60° impinge on the array with 17 sensors, with 2000 snapshots. The RMSE curves against the signal-to-noise ratio (SNR) are shown in Figs. 6 and 7 and the Cramér-Rao Bound

(CRB) is also plotted for comparison. In this case, the DOA estimation performance of the array depends on the (uniform) DOFs. It can be seen that for both the subspace based method and the sparse reconstruction based method, TS-ENA and MISC have achieved the best performance given their high uDOFs. AMDNA and D-DNA take the second place while e-PCA is the worst. This is consistent with the uDOFs provided in Table I.

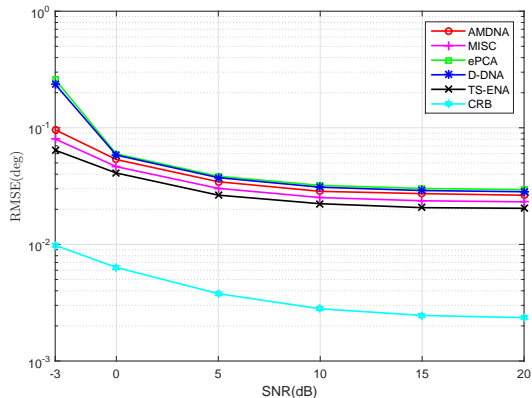


Fig. 6: RMSE of DOA estimation versus SNR in the absence of MC using TLS-ESPRIT, with $K=27$ and $T=2000$.

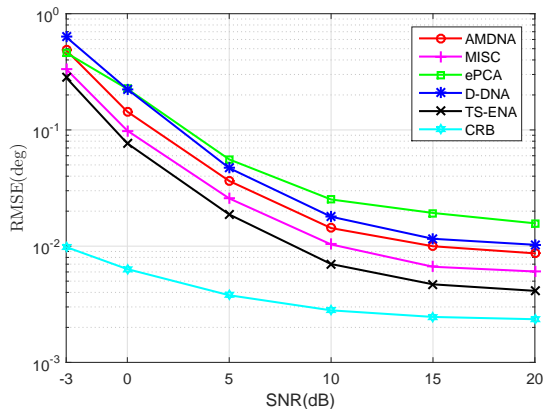


Fig. 7: RMSE of DOA estimation versus SNR in the absence of MC using LASSO, with $K=27$ and $T=2000$.

The RMSE results versus the number of snapshots using TLS-ESPRIT and LASSO are given in Fig. 8 and 9 as well as the CRB curve, where $\text{SNR}=20\text{dB}$. It is observed that in all cases, the RMSE decreases as the number of snapshots increases and that those arrays with more uDOFs exploit the increase in the number of snapshots to further improve their performance compared to the other sparse arrays with less uDOFs.

C. DOA Estimation in the Presence of Mutual Coupling

In the presence of mutual coupling, the simulation parameters are set as: 33 sources, which are uniformly distributed between -64.6° to 64.6° , impinge on the array with 28 sensors, and the number of snapshots is 2000. As shown

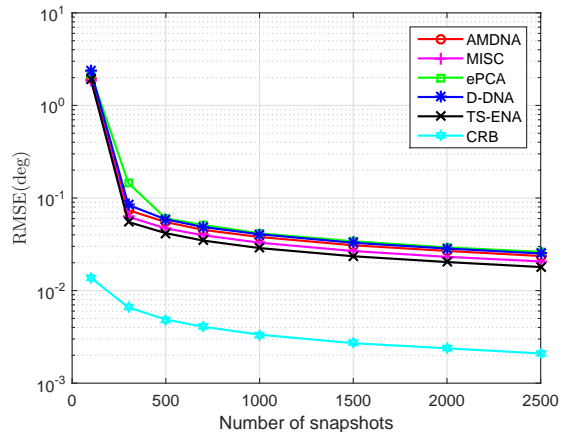


Fig. 8: RMSE versus the number of snapshots in the absence of MC using TLS-ESPRIT, with $K=27$ and $\text{SNR}=20\text{dB}$.

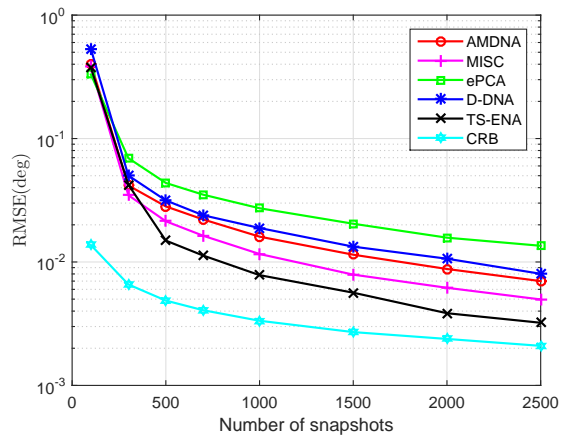


Fig. 9: RMSE versus the number of snapshots in the absence of MC using LASSO, with $K=27$ and $\text{SNR}=20\text{dB}$.

in Figs. 10 and 11, the subspace based method and sparse reconstruction based method perform a little differently. For the subspace based method, its conclusion is consistent with the one drawn in the manuscript, that is, AMDNA achieves a good balance between uDOFs and mutual coupling, thus achieving better performance than MISC and TS-ENA in strong mutual coupling situations. Note that in this case, the performance of TS-ENA with higher uDOFs but more severe coupling leakage has deteriorated significantly, which is worse than MISC. However, in the LASSO method, there are some subtle changes in the results. AMDNA still has the lowest RMSE, representing the best performance. But in this case, the performance of TS-ENA surpasses MISC at a high SNR. This might be because sparse reconstruction based methods are relatively less sensitive to mutual coupling effects, which is beneficial for TS-ENA. In both simulations, AMDNA consistently demonstrates outstanding performance across various algorithms.

The RMSE results versus the number of snapshots using TLS-ESPRIT and LASSO are plotted in Figs. 12 and 13 respectively, where $\text{SNR}=20\text{dB}$. It can be seen that the RMSEs

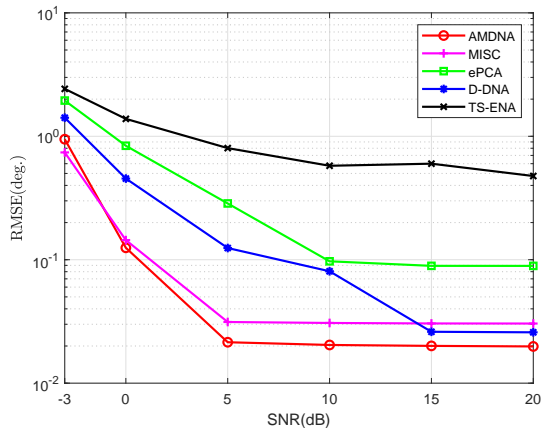


Fig. 10: RMSE of DOA estimation versus SNR in the presence of MC using TLS-ESPRIT, with $c_1 = 0.3e^{j\pi/3}$, $K=33$ and $T=2000$.

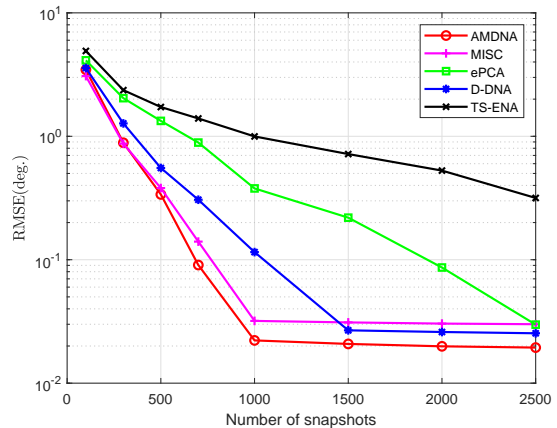


Fig. 12: RMSE versus the number of snapshots in the presence of MC using TLS-ESPRIT, with $c_1 = 0.3e^{j\pi/3}$, $K=33$ and SNR=20dB.

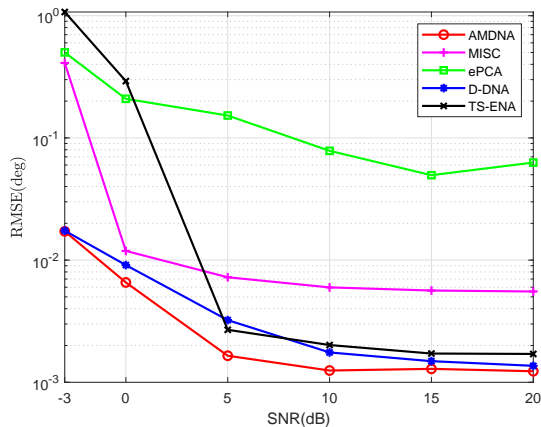


Fig. 11: RMSE of DOA estimation versus SNR in the presence of MC using LASSO, with $c_1 = 0.3e^{j\pi/3}$, $K=33$ and $T=2000$.

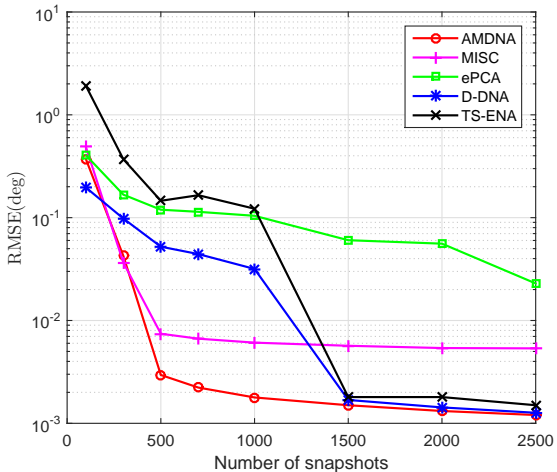


Fig. 13: RMSE versus the number of snapshots in the presence of MC using LASSO, with $c_1 = 0.3e^{j\pi/3}$, $K=33$ and SNR=20dB.

of TS-ENA decrease slowly, and AMDNA achieves the lowest RMSE, as it has both large uDOFs and low MC.

In addition, Fig. 14 illustrates the RMSE results versus the MC coefficient $|c_1|$ when SNR=20dB and $T=2000$. Along with the increase of $|c_1|$, indicating a heavy MC effect, the RMSEs of all arrays increase. In Fig. 14, when $|c_1| \leq 0.2$, it can be seen that TS-ENA performs best in all arrays, which is less sensitive to the MC effect, and meanwhile has the largest number of uDOFs. But when $|c_1| > 0.2$, TS-ENA estimation begins to degrade, and the remaining arrays tend to perform better. As seen for $|c_1| = 0.3$, AMDNA and D-DNA show an effective resistance to strong MC effects through providing accurate estimates compared to other sparse arrays. When $|c_1| = 0.4$, TS-ENA fails to provide accurate estimates due to strong MC, even though it has the largest uDOFs, while AMDNA performs best with the medium uDOFs.

To demonstrate the estimation performance of AMDNA for closely spaced DOAs, we consider 33 uncorrelated sources with an angular interval of 2 degree, and the number of sensors is 28. Then, the curve of RMSE versus SNR is provided in

Fig. 15, where $|c_1|=0.3$ and $T=2000$. It can be seen from Fig. 15 that AMDNA also enjoys the best estimation performance for closely spaced DOAs.

To further show its ability to resolve closely spaced DOAs, we also provide the curves of RMSE against the number of sources when SNR=20 dB, $|c_1|=0.3$, $T=2000$ and angle spacing is 2 degree. From Fig. 16, it can be seen that the AMDNA again has the best performance among all compared arrays.

VI. CONCLUSION

In this paper, a new systematic sparse array design scheme called MDNA has been proposed at first, which is composed of a sparse ULA and multiple identical dense ULAs with appropriate sub-ULA spacing. It is proved that the DCA of the MDNA is hole-free. For a given number of sensors with the optimal parameters, the closed-form expressions for the sensor

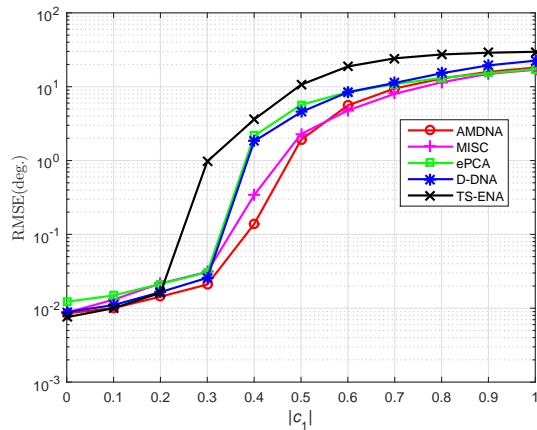


Fig. 14: RMSE versus $|c_1|$, where $K=33$, $\text{SNR}=20\text{dB}$, $T=2000$.

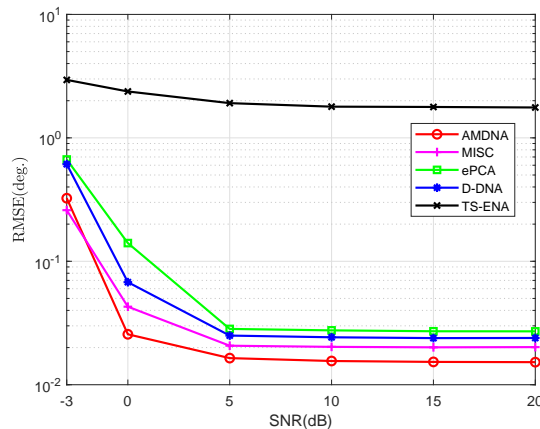


Fig. 15: RMSE versus SNR with small angle intervals (2 degree), where $c_1 = 0.3e^{j\pi/3}$ and $T=2000$.

locations and the number of uDOFs of the proposed array can be uniquely derived. More importantly, evolved from the MDNA scheme, AMDNA is proposed with less MC effects than other sparse arrays, while achieving a considerable number of uDOFs, leading to a robust DOA estimation performance. In the end, simulation results have demonstrated the effectiveness of the proposed configurations.

REFERENCES

- [1] H. Trees, *Optimum Array Processing: Part IV of Detection, Estimation, and Modulation Theory*. New York, NY, USA: Wiley, 2002.
- [2] R. Schmidt, "Multiple emitter location and signal parameter estimation," *IEEE Transactions on Antennas and Propagation*, vol. 34, no. 3, pp. 276–280, 1986.
- [3] D. Malioutov, M. Cetin, and A. Willsky, "A sparse signal reconstruction perspective for source localization with sensor arrays," *IEEE Transactions on Signal Processing*, vol. 53, no. 8, pp. 3010–3022, 2005.
- [4] M. Wang and A. Nehorai, "Coarrays, MUSIC, and the Cramer-Rao bound," *IEEE Transactions on Signal Processing*, vol. 65, no. 4, pp. 933–946, 2017.
- [5] S. Li and X.-P. Zhang, "Dilated arrays: A family of sparse arrays with increased uniform degrees of freedom and reduced mutual coupling on a moving platform," *IEEE Transactions on Signal Processing*, vol. 69, pp. 3367–3382, 2021.

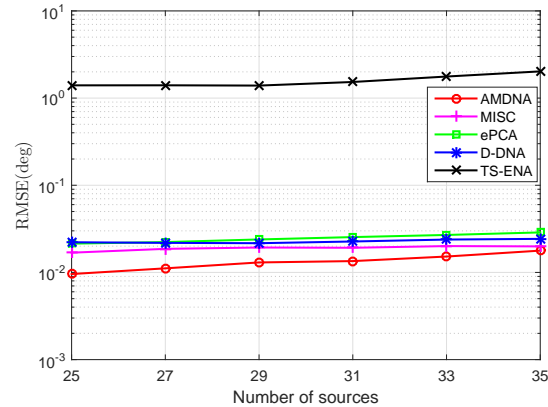


Fig. 16: RMSE versus the number of sources with small angle intervals (2 degree) in the presence of mutual coupling, where $c_1 = 0.3e^{j\pi/3}$, $\text{SNR}=20\text{dB}$ and $T=2000$.

- [6] C. Zhou, Y. Gu, Z. Shi, and M. Haardt, "Structured nyquist correlation reconstruction for DOA estimation with sparse arrays," *IEEE Transactions on Signal Processing*, pp. 1–14, 2023.
- [7] Z. Zheng, Y. Huang, W.-Q. Wang, and H. C. So, "Augmented covariance matrix reconstruction for DOA estimation using difference coarray," *IEEE Transactions on Signal Processing*, vol. 69, pp. 5345–5358, 2021.
- [8] A. Moffet, "Minimum-redundancy linear arrays," *IEEE Transactions on Antennas and Propagation*, vol. 16, no. 2, pp. 172–175, 1968.
- [9] E. Vertatschitsch and S. Haykin, "Nonredundant arrays," *Proceedings of the IEEE*, vol. 74, no. 1, pp. 217–217, 1986.
- [10] P. Pal and P. P. Vaidyanathan, "Nested arrays: A novel approach to array processing with enhanced degrees of freedom," *IEEE Transactions on Signal Processing*, vol. 58, no. 8, pp. 4167–4181, 2010.
- [11] —, "Multiple level nested array: An efficient geometry for 2 q th order cumulant based array processing," *IEEE Transactions on Signal Processing*, vol. 60, no. 3, pp. 1253–1269, 2012.
- [12] K. Han and A. Nehorai, "Improved source number detection and direction estimation with nested arrays and ULAs using jackknifing," *IEEE Transactions on Signal Processing*, vol. 61, no. 23, pp. 6118–6128, 2013.
- [13] P. P. Vaidyanathan and P. Pal, "Sparse sensing with co-prime samplers and arrays," *IEEE Transactions on Signal Processing*, vol. 59, no. 2, pp. 573–586, 2011.
- [14] J. Shi, G. Hu, X. Zhang, F. Sun, and H. Zhou, "Sparsity-based two-dimensional DOA estimation for coprime array: From sum-difference coarray viewpoint," *IEEE Transactions on Signal Processing*, vol. 65, no. 21, pp. 5591–5604, 2017.
- [15] Q. Shen, W. Liu, W. Cui, S. Wu, Y. D. Zhang, and M. G. Amin, "Low-complexity direction-of-arrival estimation based on wideband coprime arrays," *IEEE/ACM Transactions on Audio, Speech, and Language Processing*, vol. 23, no. 9, pp. 1445–1456, 2015.
- [16] C. Zhou, Y. Gu, X. Fan, Z. Shi, G. Mao, and Y. D. Zhang, "Direction-of-arrival estimation for coprime array via virtual array interpolation," *IEEE Transactions on Signal Processing*, vol. 66, no. 22, pp. 5956–5971, 2018.
- [17] Q. Shen, W. Liu, W. Cui, and S. Wu, "Underdetermined DOA estimation under the compressive sensing framework: A review," *IEEE Access*, vol. 4, pp. 8865–8878, 2016.
- [18] P. Pal and P. P. Vaidyanathan, "Coprime sampling and the MUSIC algorithm," *2011 Digital Signal Processing and Signal Processing Education Meeting (DSP/SPE)*, pp. 289–294, 2011.
- [19] S. Ren, W. Dong, X. Li, W. Wang, and X. Li, "Extended nested arrays for consecutive virtual aperture enhancement," *IEEE Signal Processing Letters*, vol. 27, pp. 575–579, 2020.
- [20] C.-L. Liu and P. P. Vaidyanathan, "Super nested arrays: Linear sparse arrays with reduced mutual coupling-Part I: Fundamentals," *IEEE Transactions on Signal Processing*, vol. 64, no. 15, pp. 3997–4012, 2016.
- [21] —, "Super nested arrays: Linear sparse arrays with reduced mutual coupling-Part II: High-order extensions," *IEEE Transactions on Signal Processing*, vol. 64, no. 16, pp. 4203–4217, 2016.
- [22] J. Liu, Y. Zhang, Y. Lu, S. Ren, and S. Cao, "Augmented nested arrays

- with enhanced DOF and reduced mutual coupling," *IEEE Transactions on Signal Processing*, vol. 65, no. 21, pp. 5549–5563, 2017.
- [23] A. M. A. Shaalan, J. Du, and Y.-H. Tu, "Dilated nested arrays with more degrees of freedom (DOFs) and less mutual coupling-Part I: The fundamental geometry," *IEEE Transactions on Signal Processing*, vol. 70, pp. 2518–2531, 2022.
- [24] S. Qin, Y. D. Zhang, and M. G. Amin, "Generalized coprime array configurations for direction-of-arrival estimation," *IEEE Transactions on Signal Processing*, vol. 63, no. 6, pp. 1377–1390, 2015.
- [25] A. Raza, W. Liu, and Q. Shen, "Thinned coprime array for second-order difference co-array generation with reduced mutual coupling," *IEEE Transactions on Signal Processing*, vol. 67, no. 8, pp. 2052–2065, 2019.
- [26] W. Zheng, X. Zhang, Y. Wang, M. Zhou, and Q. Wu, "Extended coprime array configuration generating large-scale antenna co-array in massive MIMO system," *IEEE Transactions on Vehicular Technology*, vol. 68, no. 8, pp. 7841–7853, 2019.
- [27] W. Zheng, X. Zhang, Y. Wang, J. Shen, and B. Champagne, "Padded coprime arrays for improved DOA estimation: Exploiting hole representation and filling strategies," *IEEE Transactions on Signal Processing*, vol. 68, pp. 4597–4611, 2020.
- [28] J. Shi, F. Wen, Y. Liu, Z. Liu, and P. Hu, "Enhanced and generalized coprime array for direction of arrival estimation," *IEEE Transactions on Aerospace and Electronic Systems*, pp. 1–12, 2022.
- [29] Z. Zheng, W.-Q. Wang, Y. Kong, and Y. D. Zhang, "MISC array: A new sparse array design achieving increased degrees of freedom and reduced mutual coupling effect," *IEEE Transactions on Signal Processing*, vol. 67, no. 7, pp. 1728–1741, 2019.
- [30] W. Shi, S. A. Vorobyov, and Y. Li, "ULA fitting for sparse array design," *IEEE Transactions on Signal Processing*, vol. 69, pp. 6431–6447, 2021.
- [31] W. Shi, X. Liu, and Y. Li, "ULA fitting for MIMO radar," *IEEE Communications Letters*, vol. 26, no. 9, pp. 2190–2194, 2022.
- [32] C.-L. Liu and P. P. Vaidyanathan, "Remarks on the spatial smoothing step in coarray MUSIC," *IEEE Signal Processing Letters*, vol. 22, no. 9, pp. 1438–1442, 2015.
- [33] J. Shi, Z. Yang, and Y. Liu, "On parameter identifiability of diversity-smoothing-based MIMO radar," *IEEE Transactions on Aerospace and Electronic Systems*, vol. 58, no. 3, pp. 1660–1675, 2022.
- [34] H. King, "Mutual impedance of unequal length antennas in echelon," *IRE Transactions on Antennas and Propagation*, vol. 5, no. 3, pp. 306–313, 1957.
- [35] B. Friedlander and A. Weiss, "Direction finding in the presence of mutual coupling," *IEEE Transactions on Antennas and Propagation*, vol. 39, no. 3, pp. 273–284, 1991.
- [36] B. Liao, Z.-G. Zhang, and S.-C. Chan, "DOA estimation and tracking of ULAs with mutual coupling," *IEEE Transactions on Aerospace and Electronic Systems*, vol. 48, no. 1, pp. 891–905, 2012.
- [37] Z. Ye, J. Dai, X. Xu, and X. Wu, "DOA estimation for uniform linear array with mutual coupling," *IEEE Transactions on Aerospace and Electronic Systems*, vol. 45, no. 1, pp. 280–288, 2009.